Journal of The Electrochemical Society, **152** (4) E154-E159 (2005)
0013-4651/2005/152(4)/E154/6/$7.00 © The Electrochemical Society, Inc.

Nanocrystalline Graphite for Electrochemical Sensing

Radhika C. Mani,[a] Mahendra K. Sunkara,[a,*,z] Richard P. Baldwin,[b,*] Jayadeep Gullapalli,[b] John A. Chaney,[a] Gopinath Bhimarasetti,[a,] John M. Cowley,[c] Apparao M. Rao,[d] and Rahul Rao[d]**

[a]*Department of Chemical Engineering and* [b]*Department of Chemistry, University of Louisville, Louisville, Kentucky 40292, USA*
[c]*Department of Physics and Astronomy, Arizona State University, Tempe, Arizona 85287, USA*
[d]*Department of Physics and Astronomy, Clemson University, Clemson, South Carolina 29634, USA*

We report the synthesis and characterization of a new electrode material consisting of nanocrystalline graphite (NCG) deposited onto Pt via microwave plasma chemical vapor deposition. This material exhibits stable and quasi-reversible electrochemistry for a uniquely wide range of model compounds including $Fe(CN)_6^{4-}$, $Ru(NH_3)_6^{2+}$, and selected catechols and quinones. Raman spectroscopy and electron nanodiffraction were used to confirm the presence of nanocrystals of graphite and support the hypothesis that NCG exhibits electrochemical activity similar to that of edge planes of crystalline graphite. The as-synthesized NCG material did not require any electrochemical pretreatment; however, occasionally, a one-time anodic oxidation did improve the kinetics for the catechol- and quinone-related electron transfer reactions. The electrochemical response of the electrodes was stable even after one year of storage time. The electrodes yielded clearly resolvable peaks in the voltammograms for the analytes at concentration levels similar to those in extracellular neural fluids and suggest that the electrode material may be useful for *in vivo* biological applications.
 [DOI: 10.1149/1.1870772]

Manuscript submitted May 20, 2004; revised manuscript received October 25, 2004. Available electronically March 15, 2005.

Over the last few years, there has been increasing interest in carbon-based electrodes for sensing neurological compounds. Specifically, nano-[1-3] and microcrystalline[4,5] forms of diamond and carbon nanotubes[6-10] have been investigated as alternatives to conventional pretreated glassy carbon (GC) and carbon paste materials. Thus, boron-doped microcrystalline diamond (MCD) has been shown to offer advantages over other carbon materials with respect to its low capacitance background current, wide working potential window for most solvents and electrolytes, and stable electrochemical activity without any pretreatment.[11-15] However, these properties of MCD are accompanied by a general decrease in the electrochemical reaction rates for some analytes such as catechols, compared to GC and other materials.[16] In carbon nanotubes, interesting electrochemical behavior, especially for dopamine and other biomolecules important for in vivo sensing applications, has been demonstrated;[10] and these materials certainly hold promise for electroanalysis. However, for carbon nanotubes, rapid electron transfer kinetics seems to require the presence of defect states within the graphene sheets. Hence, GC has still been attractive for the analysis of compounds such as catechols and quinones. It has been shown that the surface preparation of GC is crucial to its electrochemical performance. In particular, the surface preparation procedure, which varies widely, affects the observed electron transfer kinetics.[17] Furthermore, the activity of the prepared GC surface may also be short-lived, leading to degradation in performance and necessitating frequent reactivation. Graphite, on the other hand, is an anisotropic material, with highly reactive edge planes and nearly inert basal planes. Consequently, graphite could serve as an attractive electrode material provided that one could make predominant use of the edge planes over the basal planes. Nanocrystalline graphite (NCG) offers such a possibility. There have been a few attempts to obtain NCG using high energy laser-pulses,[18] mechanical milling,[19] ball-milling for 8 h,[20] and thermal chemical vapor deposition (CVD) from methane/hydrogen precursors.[21] However, there is little information about the possible structure of three-dimensional graphite nanocrystals; and no information has been reported so far regarding the electrochemical behavior of graphite crystals at the nanoscale.

Recently, we reported the synthesis and some preliminary observations on the electrochemical properties of a new nanocomposite carbon material prepared in a microwave plasma CVD reactor.[22] The synthesis differs from traditional CVD of diamond in that platinum wires used as substrates were placed directly into the dense plasma region to capture a high proportion of graphite and diamond nuclei. Although carbon deposition onto flat substrates using similar conditions typically yields MCD films, the high density of radicals and high temperatures (in excess of 1500 K) present at the Pt wire tip in this configuration promote the formation of NCG and diamond phases without forming amorphous sp^2 carbon. Interestingly, the electrode exhibited nearly reversible electrochemical behavior for the redox reactions of dopamine in KCl solutions.[22] However, the origin of the observed reversible electrochemical behavior was not clear. To understand the origin, extent, reproducibility, and stability of the NCG electrodes, we have synthesized a number of NCG electrodes, characterized their structure using Raman spectroscopy and nanodiffraction, and analyzed their electrochemical behavior using cyclic voltammetry (CV) with a variety of model redox compounds.

Experimental

The nanocomposite carbon films were deposited onto Pt wire substrates using a microwave plasma CVD reactor (1.5 kW ASTeX 5010). The details of the synthesis method have been described previously.[22] Figure 1 shows the schematic of the experimental setup. The platinum wires were placed vertically in the plasma with a 1-2% dilution of CH_4 in H_2 as the feed gas. Because the substrate is metallic, the entire plasma tended to discharge at the wire tip, creating very high temperatures (near the Pt melting point, 1770°C) accompanied by a high local density of gas phase species. After 24 h, nanocomposite carbon films up to 1 mm thick were deposited at the tips of the platinum wires.

These films were analyzed by micro-Raman spectroscopy with laser excitation wavelengths of 785, 514.5, and 488 nm. They were also analyzed by electron diffraction, X-ray photoelectron spectroscopy (XPS), and X-ray diffraction (XRD).

Surface compositional analysis of the electrodes was performed with XPS using Al Kα X-rays (λ = 8.34 Å) and a spectrometer pass energy of 50 meV. The small size of the electrode tips necessitated bundling three electrodes together to obtain adequate sampling signal. A fresh plasma-cleaned Si(100) surface served as a support for the bundle, and a spectrum of identically treated Si(100) was used as a blank to account for carbon and/or oxygen contributions from the support. The C(1s) and O(1s) spectral windows from the blank were subtracted from the observed C(1s) and O(1s)

* Electrochemical Society Active Member.
** Electrochemical Society Student Member.
z E-mail: mahendra@louisville.edu

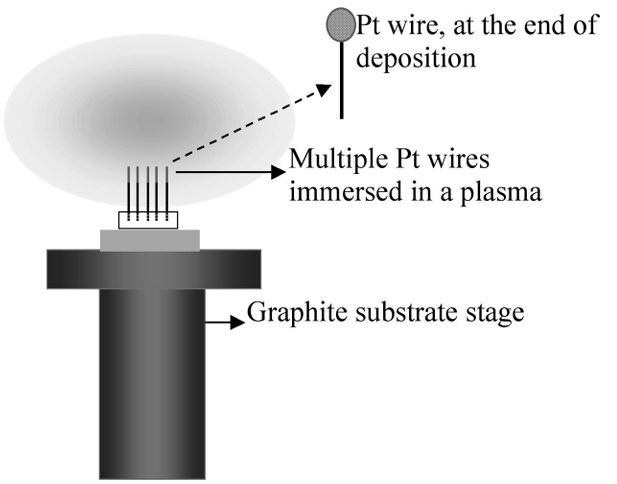

Figure 1. A schematic of the synthesis of multiple electrodes containing the nanocomposite material.

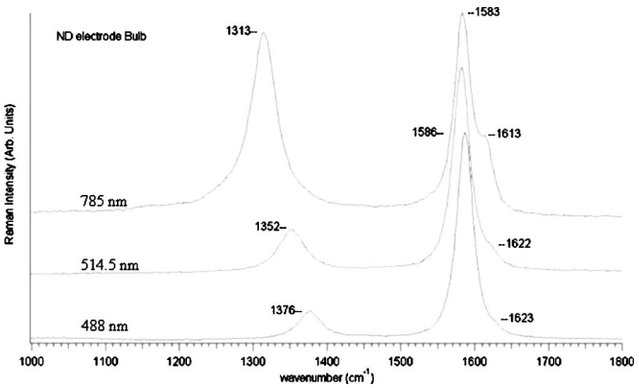

Figure 2. Micro-Raman spectra taken from the bulb-shaped nanocomposite deposit using different laser excitation wavelengths of 785, 514.5, and 488 nm.

features of the supported electrodes. In this way, the XPS data obtained were representative of only the nanocomposite carbon surfaces.

CV experiments were carried out with a Bioanalytical Systems model CV-50W Voltammetric Analyzer equipped with a single-compartment, three-electrode cell with Ag/AgCl (3 M KCl) reference and Pt wire auxiliary electrodes. The area (geometrical and electrochemical) varied with each electrode and was determined approximately. In some CV experiments, GC and MCD electrodes were employed for comparison purposes. GC electrodes were obtained from Bioanalytical Systems (model MF-2012, 3.0 mm diameter), while MCD electrodes were prepared in our own lab. CVs of the nanocomposite diamond deposits were obtained by immersing the head of the electrode (ball-shaped) into the solution while blanking the rest of the electrode with an insulating enamel to ensure the electrochemical response originated only from the nanocomposite material. Most of the analytes, serotonin (5-hydroxytyramine), uric acid, ascorbic acid, dopamine, potassium ferricyanide ($K_3(Fe(CN)_6)$), catechol, 4-methyl catechol, and ruthenium hexamine hydrochloride, were obtained from Sigma-Aldrich. CVs were usually run in 0.10 M KCl electrolyte, but a 0.20 M phosphate buffer solution was used occasionally to maintain a pH of 7. Deaerating the solutions with N_2 had little effect on the observed CVs. Room-temperature electrode impedance spectroscopy (EIS) was performed with a model 273A Princeton Applied Research Potentiostat/Galvanostat in 0.10 M KCl solution.

Results and Discussion

Material characterization.—Multiple platinum wires were placed vertically into the CVD growth system with only the tips immersed in the dense plasma region, as illustrated in Fig. 1. After 24 h of deposition, a dense ball-shaped deposit of carbon formed at the tip. This deposit, which was characterized with surface spectroscopy and electrochemistry as described below, was the primary focus of this investigation. Note that when similar platinum wires were placed horizontally in the low-temperature region of the plasma, a uniform MCD deposit was formed on the platinum wire as expected.

Raman spectra taken at different wavelengths on the nanocomposite material are presented in Fig. 2. A number of studies have indicated that the presence of the two peaks, one around 1350 cm^{-1} and the other around 1580 cm^{-1}, is clearly indicative of D and G bands of graphite, respectively.[23] An additional peak at 1620 cm^{-1} is indicative of the D′-band.[24] The D and D′-band arise due to disorder in the graphite, *i.e.*, perfect graphite sheets would yield only the G band.[23] Interestingly, the Raman spectrum (785 nm excitation) shown in Fig. 2 exhibits peaks matching each of these band locations. However, the broad shoulder between 1350 and 1550 cm^{-1} that is normally attributed to the amorphous sp^2 carbon phase[25-28] is clearly absent in our spectra.

Raman spectroscopy is very sensitive to the presence of sp^2 carbon in comparison to sp^3 carbon.[29] In particular, both the position and the intensity of the D-band depend on the crystallite size and the laser excitation wavelength. With decreased excitation wavelength, D-bands shift to higher wave numbers and decrease in intensity.[30] Thus, for materials potentially containing both diamond and graphite crystalline phases, short laser wavelengths (~244 nm) must ideally be used to distinguish between the diamond signature at 1332 cm^{-1} band and the D-band close to 1350 cm^{-1}.[31] In this study, we expanded upon our earlier Raman observations by using excitation wavelengths of 785, 514, and 488 nm as shown in Fig. 2. Decreasing the wavelength from 785 to 488 nm shifts the D-band from 1313 to 1376 cm^{-1}, while the G-band at 1583 cm^{-1} remains relatively constant, consistent with other reports for sp^2 graphite.[23,30-32] On this basis, we believe that our earlier assignment[22] of the 1314 cm^{-1} peak to nanocrystalline diamond was incorrect.

According to Knight's formula, the relation between the ratio of the D/G band intensity and the graphite cluster size[23,30,32] is

$$La = (I_G/I_D) \quad [1]$$

where L_a is the graphite cluster size, I_G and I_D are the G- and D-band intensities, and C is a wavelength dependent term. If one were to use the linear dependence of C on wavelength suggested by Matthews *et al.*[30] in the range 400-785 nm, the value of C for a wavelengths of 633 and 785 nm would be ~83 and ~133 Å, respectively. The integrated intensity ratio (I_G/I_D) calculated for our nanocrystalline material at laser excitation wavelengths 633 nm was 1.147 (data not shown) and at 785 nm was 0.68.[22] Using Knight's formula, the crystallite size obtained for our nanocomposite material can be estimated as less than 10 nm. We obtained a similar crystal size for 514 and 488 nm laser wavelengths. As the expected penetration depth for a Raman laser with wavelength 785 nm is less than 1 μm, this indicates that at least the surface of the nanocomposite material is dominated by nanocrystals of graphite.

Nanodiffraction studies were also performed on 1 nm regions of the ball-shaped tip of the CVD-deposited material. When such a bulb was taken intact and mounted on a grid, scanning tunneling electron microscopy (STEM) observations indicated that the bulb was relatively smooth, with small hills on it, and gave graphite diffraction patterns consistent with the basal plane oriented roughly parallel to the surface. The dark field images of the nanocrystals along with their corresponding electron nanodiffraction patterns (taken from 1 nm regions) are shown in Fig. 3. These images show

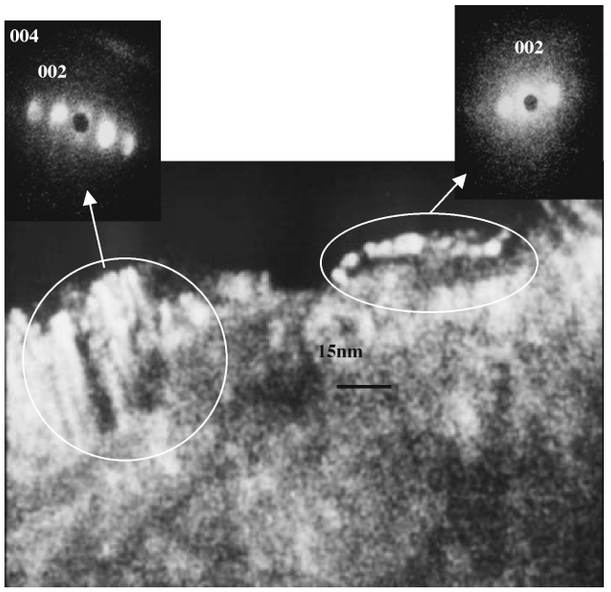

Figure 3. Dark field image taken from the intact bulb-part of the electrode. The surface show low hills of graphite nanocrystals. The electron nanodiffraction patterns (insets) are taken approximately from regions about 1 nm within the areas indicated.

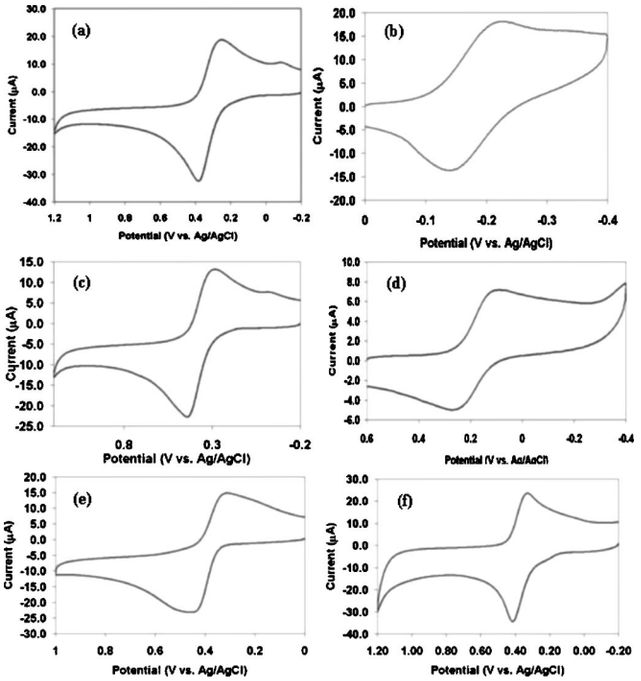

Figure 4. CV of 1 mM (a) 4-Methyl catechol, (b) Ruthenium hexamine hydrochloride, (c) Catechol, (d) Ferricyanide, (e) Hydroquinone, and (f) Dopamine in 0.1 M KCl solution at 100 mV/s scan rate. Electrode area is 0.03 cm^2.

that the graphite crystals were often only as small as 10 nm in diameter and had sharp edges. Also, the diffraction patterns showed abrupt changes in lattice orientation between the crystallites. These observations regarding the graphite crystallite size and structure were in substantial agreement with the Raman analysis presented above.

The right hand inset in Fig. 3 shows only strong first order reflections that are indicative of the presence of very small distorted crystals. This may be due to the presence of many exposed graphite edge planes. When the samples were crushed and the resulting bulk material was analyzed by STEM, almost a third of the crystallites appeared to be graphitic. In addition, there was a significant amount of amorphous material but only a very small proportion of diamond phase present. Furthermore, the diamond crystals present were mostly embedded within the amorphous matrix and therefore were not deemed likely to be responsible for any of the observed electrochemical behavior. As a check, XRD (not shown) was performed on the material scraped from the surface of the electrode. The XRD revealed a clear feature associated with the (002) graphite plane with a size estimate (using full-width at half-maximum) again on the order of 10 nm.

Our conclusions based on the Raman, electron nanodiffraction, and XRD studies was that the surface of our nanocomposite material is dominated by NCG with a crystallite size of ~10 nm.

Electrochemical studies.—It is generally accepted that the edge plane of graphite is much more reactive towards electron transfer and adsorption than the basal plane. In view of the fact that our as-synthesized material contains substantial NCG and should therefore have an unusually high proportion of edge planes, we expected that it might be an interesting electrode material with especially good electron transfer characteristics. Our initial communication[22] confirmed that this was the case for dopamine oxidation and encouraged us to explore the voltammetry of a broad range of redox compounds at an NCG electrode.

Figure 4a-f shows the CVs obtained using the NCG material for a series of model electroactive analytes. 0.10 M KCl was used as the electrolyte because this has been frequently reported in the literature for these compounds with GC and MCD electrodes. The specific peak separation values (ΔEp) seen in this figure for NCG are listed in Table I and compared with those obtained under identical solution conditions for untreated GC and MCD. In comparison to the near-reversible response seen at the NCG electrode, both untreated GC and MCD gave much less reversible behavior for most of the analytes. These results illustrate that NCG clearly represents an interesting electrode material for electroanalytical applications.

A series of tests were employed on several electrodes to gain more insight into the electrochemical activity of the NCG. The electrodes were tested with regard to stability, nature of surface sites, and selectivity in mixtures of analytes. In all these tests, we used dopamine as the model analyte which, due to its physiological importance, has been extensively studied on several types of carbon-based electrodes.[33,34]

As shown in Fig. 4f, the as-synthesized NCG electrodes typically showed a quasi-reversible peak separation for dopamine without any pretreatment with ΔEp ~ 100 mV in 0.10 M KCl. However, a few

Table I. Comparison of the ΔE_p values obtained using CVs for different analytes at untreated GC, MCD and the NCG electrode material.[a]

Compounds	GC	MCD	NCG
4-Methyl catechol	0.49 V	1.06 V	0.13 V
$Ru(NH_3)_6^{2+}$	0.07 V	0.09 V	0.08 V
Catechol	0.55 V	1.02 V	0.14 V
$Fe(CN)_6^{3+}$	0.5 V	0.65 V	0.08 V
Hydroquinone	0.55 V	1.2 V	0.21 V
Dopamine	0.65 V	1.0 V	0.12 ± 0.02 V
Ascorbic Acid	1.2 V[b]	1.6 V[b]	0.21 V[b]

[a] ΔE_p values were obtained for 1.0 mM concentrations in 0.10 M KCl solution at a potential scan rate of 100 mV/s.

[b] Oxidation was irreversible at all electrode materials; therefore, values shown here are the E_c potentials seen for ascorbic acid oxidation at each electrode.

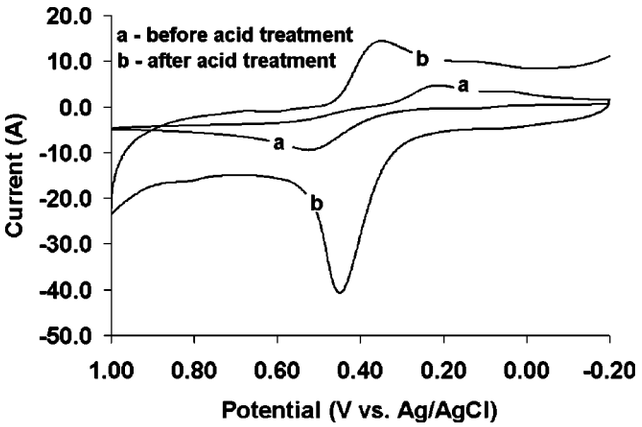

Figure 5. The CV of 1 mM Dopamine in 0.1 M KCl at 100 mV/s scan rate before and after acid treatment. Acid treatment consisted of scanning the electrode from −2.0 to + 2.0 V *vs.* Ag/AgCl in 0.50 M H_2SO_4 for two cycles.

of the electrodes (~1 in 5) required anodic oxidation at +2.0 V in 0.5 M H_2SO_4 to reduce the ΔEp for dopamine in 0.1 M KCl from 350 mV to a nearly reversible 100 mV (see Fig. 5). Interestingly, this decrease in peak separation was also accompanied by a general increase in the background current, which was mainly due to an increase in the active surface sites (as explained below). Most important, these electrodes, after the one-time anodic oxidation treatment, and the remaining electrodes, without any treatment, exhibited stable and reversible response with usage over the entire period of this study, *i.e.*, over a year. ΔEp of about 10 electrodes for 1 mM dopamine in 0.10 M KCl was 0.12 V ± 0.02 V. Additionally, the plot of the anodic current *vs.* the square root of the scan rate gave a linear dependence over a wide range (figure not shown). This indicates that the overall electrochemical process for dopamine at the NCG electrodes is diffusion-controlled.

EIS measurements indicated that the capacitance of the as-synthesized NCG material was about 5.5 μF for 0.03 cm^2 electrochemical area or roughly 180 $\mu F/cm^2$ which is substantially greater than that reported for MCD (0.05-5 $\mu F/cm^2$),[11] GC (25 -30 $\mu F/cm^2$),[11] and edge-plane graphite (70 $\mu F/cm^2$).[35] The effective electrochemical area of the NCG electrodes was calculated from the slope of the cathodic peak current (diffusion-limited current) *vs.* square root of scan rate for a 1 mM solution of $K_3Fe(CN)_6$. The high value for the specific capacitance of NCG could presumably be due to the higher concentrations of graphite edge planes on the electrode surface. Significant presence of graphite edge planes can lead to faster kinetics and hence increased accumulation of surface charge.

McCreery's pioneering studies demonstrated that the electron transfer kinetics increases with increasing adsorption of catechols on GC surfaces.[36] There are several ways by which dopamine can adsorb on the surface of carbon electrodes. One adsorption pathway is through oxygen functionalization of the surface, *e.g.*, the formation of -COOH or -C = O due to anodic oxidation on the surface of diamond[13] or GC[34] and the subsequently increased interactions between these groups and the catechol compound. Electron transfer then occurs from the species in the solution to a surface already saturated with adsorbed redox species.[36] The second pathway of increased adsorption of catechols is by means of surface defect sites on graphite.[37] Therefore, surface spectroscopy was used to identify surface functionalities in order to determine which of the above pathways was primarily responsible for the quasi-reversible behavior seen for dopamine at NCG.

XPS analysis was performed both on as-synthesized NCG electrodes that provided an immediate reversible response to dopamine

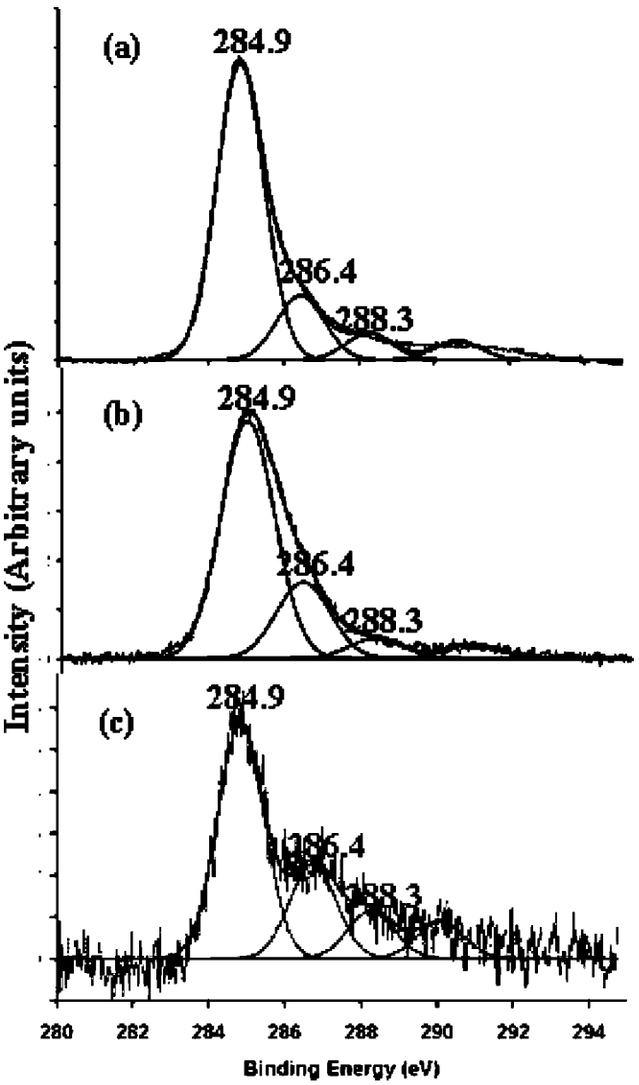

Figure 6. XPS spectra taken on the (a) as-synthesized well-working NCG electrode (b) as-synthesized NCG electrode with irreversible behavior (c) after anodic oxidation of (b) in 0.5 M H_2SO_4 at 2.0 V, indicating an increase in groups corresponding to 284.9, 286.4, 288.3 eV.

and on nonideal NCG electrodes (before and after electrochemical anodization) that showed slight irreversibility when used as synthesized. The C(1s) XPS spectra for such electrodes is presented in Fig. 6. Of course, absolute quantification of oxide functionalities on the surface was difficult due to the extremely small area of the electrode in comparison to the region over which each spectrum was taken; and a simple Gaussian deconvolution model was used to analytically extract spectral features. As shown in Fig. 6, the three main features seen following deconvolution consisted of peaks at 284.9, 286.4, and 288.3 eV, which have been interpreted elsewhere as C-C graphite carbon ring, C-OH, and C = O, respectively.[38,39] These results are summarized numerically in Table II where it can be seen that the amount of carbonyl functional group increased significantly following the oxidation treatment [column (b) *vs.* (c)] as has been previously reported for GC,[40] graphite,[35,41] and diamond.[12,42] However, the electrodes that showed good initial performance before any electrochemical treatment exhibited a smaller proportion of oxygen-containing functional groups than either of the other surfaces [column (a) *vs.* (b) and (c)]. Hence, the oxygen-containing surface species clearly did not seem to be directly associated with the re-

Table II. Deconvoluted C(1s) spectrum and percentage composition

Peak position/ assignment	(a) Electrode with reversible response	(b) Electrode with irreversible response	(c) Electrode (b) anodically oxidized
284.9 eV-graphitic (C=C)	76.4	71	62
286.4 eV-alcoholic (-OH)	16.7	22.8	25.3
288.3 eV-carbonyl (-C=O)	6.9	6.2	12.7

versible electrochemical behavior observed for the NCG material.

Interestingly, the estimated electrochemical area nearly doubled after electrochemical anodization. Further, the capacitance of the material, determined using EIS, also increased dramatically from $\sim$5.5 to $\sim$ 80 μF for the same electrode after two successive anodic oxidations (but did not increase significantly further). Also, successive anodic oxidations did not decrease further the ΔEp value for dopamine redox couple. Thus, we speculate that the NCG electrodes displaying poor performance on initial CV experimentation may have had larger grain sizes or perhaps had edge planes that were bent and hence not directly exposed to the solution. Thus, they did not give a very reversible response for dopamine initially. Previously, McCreery showed that oxidation of the surface by electrochemical treatment creates defects on graphite,[37] which may in turn increase the reactivity as noted earlier. The observed increases in capacitance and electrochemically active surface sites lend support to the hypothesis that the electrochemical anodization here creates a large number of such surface defect sites. In comparison, when MCD was anodically treated, an increase in oxygen containing functional groups on the surface has likewise been reported.[4] However, the diamond surface, which is comparatively inert to adsorption, continued to give a highly irreversible peak for the dopamine redox processes even when terminated by oxygen-containing functional groups after anodization.[4,43]

The NCG electrode performance, with or without electrochemical pretreatment, was quite stable over a long period of time. One electrode was tested with daily usage over a month and the resulting CV performance with dopamine is presented in Fig. 7. As shown by Fig. 7, the ΔEp had a negligible change over this period. The background and peak current did change, while maintaining the same signal-to-background ratio, because the exposed electrode area

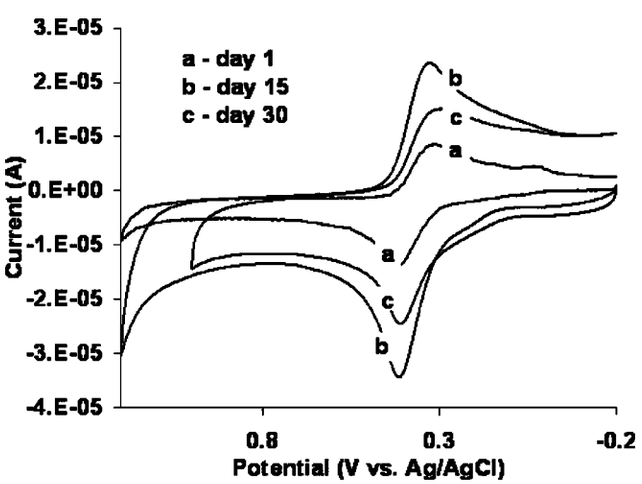

Figure 7. CV of 1 mM dopamine in 0.1 M KCl at 100 mV/s scan rate on the same electrode over a period of 1 month when the electrode was being used regularly.

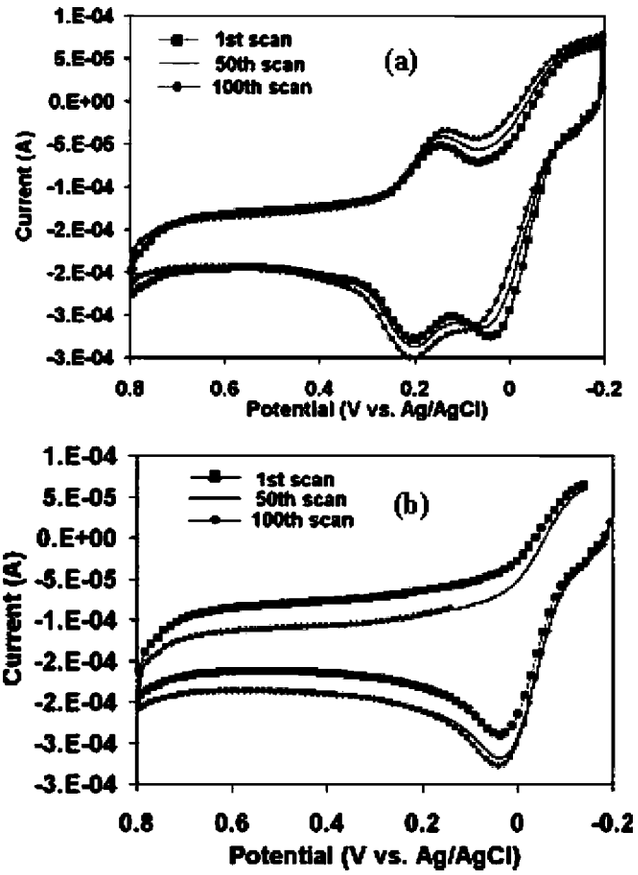

Figure 8. CV obtained after anodic oxidation during continuous scanning at 100 mV/s at pH 7 phosphate buffer solution containing (a) 10 mM of Ascorbic acid, 0.10 mM dopamine mixture, and (b) 10 mM ascorbic acid.

could not be kept exactly the same each time the CV was taken. This stable behavior is similar to that seen for MCD but is seems much better than GC, which requires frequent reactivation of the surface to overcome sluggish kinetics.

Neurotranmitter applications.—In the *in vivo* neural environment, the extracellular fluid that serves as the sample matrix contains an excess of ascorbic acid and comparatively small amounts of dopamine, DOPAC, serotonin, etc. Therefore, it is desirable to have an electrode material that can clearly resolve the peaks for all the analytes present in this mixture. Also, as the pH of the neurological environment is close to 7 and the oxidation potential of dopamine is quite sensitive to pH, it was appropriate to carry out subsequent CV experiments in buffered solution (in this case, 0.20 M pH 7 phosphate buffer). Interestingly, CV with the as-synthesized NCG electrodes, lacking acid pretreatment, could not distinguish between ascorbic acid and dopamine as both compounds gave oxidation waves at $\sim$0.2 V (*vs.* Ag/AgCl) under these conditions. However, a single anodic treatment in 0.5 M H_2SO_4 produced the CV shown in Fig. 8 where two readily distinguishable oxidations can be seen for ascorbic acid and dopamine. This occurred because the anodic oxidation treatment shifted the irreversible ascorbic acid oxidation process to lower potentials but did not change the position of the nearly reversible dopamine redox couple. A similar effect has been observed for anodically oxidized graphite-epoxy electrodes[44] and for vacuum heat-treated GC.[45] Contrary to this result, at the surface of MCD, the oxidation peak for ascorbic acid shifts to higher potentials upon anodic pre-treatment.[4] In addition, comparing the results in Fig. 4f obtained using unbuffered 0.1 M KCl solution (pH 5-6) to those obtained with pH 7 phosphate buffer, the anodic peak position

shifted by 0.2 V and the peak separation decreased for the buffered system. This phenomenon is consistent with a prior detailed study of dopamine reaction kinetics on a carbon electrode which showed that the anodic peak position shifts differently than the cathodic peak position with pH.[46] Our observations of 200 mV shift in E_a for the dopamine redox couple using our electrode material could possibly be caused by the difference in pH values of the unbuffered KCl and phosphate buffer solutions used, although other explanations are possible.

As discussed previously, XPS analysis indicates that the anodic treatment introduces oxygen functionalities at the NCG surface. These oxygen functionalities presumably catalyzed the oxidation of ascorbic acid, shifting its oxidation potential to lower values. As shown in Fig. 8, continuous scanning of the electrode after anodic oxidation did not change the response of ascorbic acid even after more than a hundred scans. The exact oxide species catalyzing the ascorbic acid oxidation on our electrode surface is a subject of further investigations. However, the results in Fig. 8 indicate the possible use of the NCG electrode to detect *in vivo* concentrations of dopamine in the presence of excess ascorbic acid.

Conclusions

A novel NCG electrode material was synthesized onto platinum wire substrates by placing them directly into the dense, high temperature region of a 2-4% CH_4/H_2 plasma. The resulting NCG films gave CV behavior that was fundamentally different from that seen at other carbon electrode materials including both glassy carbon and diamond. In particular, it exhibited reversible or quasi-reversible kinetics for several model electron transfer processes. This was attributable, we believe, to the presence of a high density of exposed and reactive edge sites in the as-synthesized NCG material. This hypothesis was supported by Raman, XPS, and X-ray and electron diffraction measurements. Other attractive features of this NCG material are its ease of synthesis and its stability for extended periods of usage. The NCG material presents an interesting possibility for electroanalytical detection of neurotransmitters *in vivo*.

Acknowledgments

Financial support from the National Science Foundation through CAREER grant (CTS 9876251) and Infrastructure program (EPS 0083103) is gratefully appreciated.

The University of Louisville assisted in meeting the publication costs of this article.

References

1. Y. Show, M. A. Witek, P. Sonthalia, and G. M. Swain, *Chem. Mater.*, **15**, 879 (2003).
2. L. C. Hian, K. J. Grehan, R. G. Compton, J. S. Foord, and F. Marken, *J. Electrochem. Soc.*, **150**, E59 (2003).
3. Q. Y. Chen, D. M. Gruen, A. R. Krauss, T. D. Corrigan, M. Witek, and G. M. Swain, *J. Electrochem. Soc.*, **148**, E44 (2001).
4. E. Popa, H. Notsu, T. Miwa, D. A. Tryk, and A. Fujishima, *Electrochem. Solid-State Lett.*, **2**, 49 (1999).
5. M. C. Granger, M. Witek, J. S. Xu, J. Wang, M. Hupert, A. Hanks, M. D. Koppang, J. E. Butler, G. Lucazeau, M. Mermoux, J. W. Strojek, and G. M. Swain, *Anal. Chem.*, **72**, 3793 (2000).
6. J. Koehne, J. Li, A. M. Cassell, H. Chen, Q. Ye, H. T. Ng, J. Han, and M. Meyyappan, *J. Mater. Chem.*, **14**, 676 (2004).
7. F. Valentini, A. Amine, S. Orlanducci, M. L. Terranova, and G. Palleschi, *Anal. Chem.*, **75**, 5413 (2003).
8. Z. H. Wang, J. Liu, Q. L. Liang, Y. M. Wang, and G. Luo, *Analyst (Cambridge, U.K.)*, **127**, 653 (2002).
9. J. M. Nugent, K. S. V. Santhanam, A. Rubio, and P. M. Ajayan, *Nano Lett.*, **1**, 87 (2001).
10. W. C. Poh, K. P. Loh, W. D. Zhang, S. Triparthy, J.-S. Ye, and F.-S. Sheu, *Langmuir*, **20**, 5484 (2004).
11. J. Xu, M. C. Granger, Q. Chen, J. W. Strojek, T. E. Lister, and G. M. Swain, *Anal. Chem.*, **69**, 591A (1997).
12. H. B. Martin, A. Argoitia, U. Landau, A. B. Anderson, and J. C. Angus, *J. Electrochem. Soc.*, **143**, L133 (1996).
13. H. B. Martin, A. Argoitia, J. C. Angus, and U. Landau, *J. Electrochem. Soc.*, **146**, 2959 (1999).
14. G. M. Swain, A. B. Anderson, and J. C. Angus, *MRS Bull.*, **23**, 56 (1998).
15. R. Tenne and C. Levy-Clement, *Isr. J. Chem.*, **38**, 57 (1998).
16. Y. V. Pleskov, *Russ. J. Electrochem.*, **38**, 1411 (2002).
17. P. H. Chen and R. L. McCreery, *Anal. Chem.*, **68**, 3958 (1996).
18. T. Dallas, M. Holtz, H. Ahn, and M. C. Downer, *Phys. Rev. B*, **49**, 796 (1994).
19. K. Itoh, Y. Miyahara, S. Orimo, H. Fujii, T. Kamiyama, and T. Fukunaga, *J. Alloys Compd.*, **356**, 608 (2003).
20. T. D. Shen, W. Q. Ge, K. Y. Wang, M. X. Quan, J. T. Wang, W. D. Wei, and C. C. Koch, *Nanostruct. Mater.*, **7**, 393 (1996).
21. J. R. Patterson, A. Kudryavtsev, and Y. K. Vohra, *Appl. Phys. Lett.*, **81**, 2073 (2002).
22. R. C. Mani, S. Sharma, M. K. Sunkara, J. Gullapalli, R. P. Baldwin, R. Rao, A. M. Rao, and J. M. Cowley, *Electrochem. Solid-State Lett.*, **5**, E32 (2002).
23. F. Tuinstra and J. L. Koenig, *J. Chem. Phys.*, **53**, 1126 (1970).
24. G. Katagiri, H. Ishida, and A. Ishitani, *Carbon*, **26**, 4 (1988); **26**, 565 (1988).
25. S. Prawer, K. W. Nugent, and D. N. Jamieson, *Diamond Relat. Mater.*, **7**, 106 (1998).
26. Z. Sun, J. R. Shi, B. K. Tay, and S. P. Lau, *Diamond Relat. Mater.*, **9**, 1979 (2000).
27. J. D. Hunn, S. P. Withrow, C. W. White, and D. M. Hembree, *Phys. Rev. B*, **52**, 8106 (1995).
28. A. K. Arora, T. R. Ravindran, G. L. N. Reddy, A. K. Sikder, and D. S. Misra, *Diamond Relat. Mater.*, **10**, 1477 (2001).
29. R. J. Nemanich, J. T. Glass, G. Lucovsky, and R. E. Shroder, *J. Vac. Sci. Technol. A*, **6**, 1783 (1988).
30. M. J. Matthews, M. A. Pimenta, G. Dresselhaus, M. S. Dresselhaus, and M. Endo, *Phys. Rev. B*, **59**, R6585 (1999).
31. S. M. Huang, Z. Sun, Y. F. Lu, and M. H. Hong, *Surf. Coat. Technol.*, **151-152**, 263 (2002).
32. A. C. Ferrari and J. Robertson, *Phys. Rev. B*, **61**, 14095 (2000).
33. M. R. Deakin and R. M. Wightman, *J. Electroanal. Chem. Interfacial Electrochem.*, **206**, 167 (1986).
34. G. E. Cabaniss, A. A. Diamantis, W. R. Murphy, R. W. Linton, and T. J. Meyer, *J. Am. Chem. Soc.*, **107**, 1845 (1985).
35. R. J. Rice and R. L. McCreery, *Anal. Chem.*, **61**, 1637 (1989).
36. S. H. Du Vall and R. L. McCreery, *J. Am. Chem. Soc.*, **122**, 6759 (2000).
37. R. Bowling, R. T. Rackard, and R. L. McCreery, *Langmuir*, **5**, 683 (1986).
38. R. H. Bradley, X. Ling, and I. Sutherland, *Carbon*, **31**, 1115 (1993).
39. S. Biniak, G. Szymanski, J. Siedlewski, and A. Swaitowski, *Carbon*, **35**, 1799 (1997).
40. M. Nakahara, Y. Nakayama, G. Katagiri, and K. Shimizu, *J. Mater. Sci.*, **26**, 861 (1991).
41. F. Regisser, M. A. Lavoie, G. Y. Champagne, and D. Belanger, *J. Anal. Chem. USSR*, **415**, 47 (1996).
42. H. Notsu, I. Yagi, T. Tatsuma, D. A. Tryk, and A. Fujishima, *J. Electroanal. Chem.*, **492**, 31 (2000).
43. B. V. Sarada, T. N. Rao, D. A. Tryk, and A. Fujishima, *Anal. Chem.*, **72**, 1632 (2000).
44. L. Falat and H. Y. Cheng, *Anal. Chem.*, **54**, 2111 (1982).
45. I. F. Hu and T. Kuwana, *Anal. Chem.*, **58**, 3235 (1986).
46. K. T. Kawagoe, P. A. Garris, and R. M. Wightman, *J. Electroanal. Chem.*, **359**, 193 (1993).